

Large signal RF power transmission characterization of InGaP HBT for RF power amplifiers

Zhao Lixin(赵立新)[†], Jin Zhi(金智), and Liu Xinyu(刘新宇)

(Institute of Microelectronics, Chinese Academy of Sciences, Beijing 100029, China)

Abstract: The large signal RF power transmission characteristics of an advanced InGaP HBT in an RF power amplifier are investigated and analyzed experimentally. The realistic RF powers reflected by the transistor, transmitted from the transistor and reflected by the load are investigated at small signal and large signal levels. The RF power multiple frequency components at the input and output ports are investigated at small signal and large signal levels, including their effects on RF power gain compression and nonlinearity. The results show that the RF power reflections are different between the output and input ports. At the input port the reflected power is not always proportional to input power level; at large power levels the reflected power becomes more serious than that at small signal levels, and there is a knee point at large power levels. The results also show the effects of the power multiple frequency components on RF amplification.

Key words: large signal characteristics; InGaP HBT; nonlinearity

DOI: 10.1088/1674-4926/31/1/014001

PACC: 7280E; 7360L

1. Introduction

Advanced indium gallium phosphide heterojunction bipolar transistors (InGaP HBTs) are key components in RF power amplifiers in radar and communication systems^[1–3]. RF power amplifiers in communication and radar systems are usually used for linear power amplifications. However, this situation will not be met at large power levels. At large signal power levels the transistors show complicated characteristics^[4–6]. So, practical large signal characterization will be of benefit to RF power amplifier design^[7, 8].

Unlike time domain waveform analysis, in this paper the RF large signal power transmission characteristics of an advanced InGaP HBT cell are investigated for 5.8 GHz amplifier applications. Firstly, realistic RF powers injected to and reflected by the transistor, transistor transmitted power and load reflected power are investigated and analyzed at small signal and large signal levels. Then the power multiple frequency components are analyzed, and the major factors affecting power gain and linearity are analyzed at small signal levels, at the -1 dB gain compression point, at the -3 dB gain compression point, and at the maximum saturation output power point. Finally, the large signal RF power transmission characteristics and the RF power multiple frequency component effects on power gain and linearity are summarized.

2. RF power transmission characterization

In this investigation, the amplifier transistor is an InGaP/GaAs npn transistor cell with a device area around 1×10^{-3} mm². The transistor DC current gain is $\beta = 80$, and the collector–emitter breakdown voltage is about 12 V. The transistor maximum oscillation frequency is around 110 GHz, and the cutoff frequency is about 40 GHz. The transistor was measured on wafer using by PicoProbe ground-signal-ground (GSG) probes and a Cascade test station in an AgilentN5242

nonlinear vector network analyzer system^[9, 10], and for maximum output power at initial bias conditions of $V_{CE} = 3.61$ V, $I_C = 53.7$ mA, $V_{BE} = 1.28$ V, $I_B = 0.71$ mA.

With the injection of a sinusoidal RF signal and increasing the input power level, the injection power, the reflected power to the transistor, the transmitted power from the transistor, and the reflected power from the load are investigated at small signal injection levels, at the -1 dB gain compression point $P_{-1\text{dB}}$, at the -3 dB gain compression point $P_{-3\text{dB}}$, and at the maximum saturation output power point P_{sat} in the following subsections.

2.1. RF power transmission at output port

At small signal injection levels, a sinusoidal RF signal with a power of -8.64 dBm at frequency $f_0 = 5.8$ GHz is injected to the transistor. At the output port the transmitted power from the transistor is about 6.88 dBm, and the reflected power from the load is about -5.06 dBm. On increasing the injection power from a small signal to 5.0 dBm, -1 dB gain compression point, the transmitted power is 19.26 dBm, and the power reflected by the load is about 7.30 dBm at the output port. On increasing the injection power from the -1 dB gain compression point to 8 dBm, -3 dB gain compression point, the transmitted power is 20.57 dBm and the reflected power is 8.6 dBm at the output port. On increasing the injection power from the -3 dB gain compression point to 16.5 dBm, power saturation point, the transmitted power reaches 21.5 dBm and the power reflected by the load is 9.5 dBm at output. Figure 1 shows the transmitted power and reflected power.

Obviously the reflected power is in proportion to the transmitted power not only at the small signal level, but also at the -1 dB gain compression point, at the -3 dB gain compression point, and at the saturation output power point. The reflected power is about 12 dB lower than the transmitted power at small signal and large signal levels. The reflected powers only occupy a small part of the transmitted power.

[†] Corresponding author. Email: zhaolixin@ime.ac.cn

Received 20 July 2009, revised manuscript received 20 August 2009

© 2010 Chinese Institute of Electronics

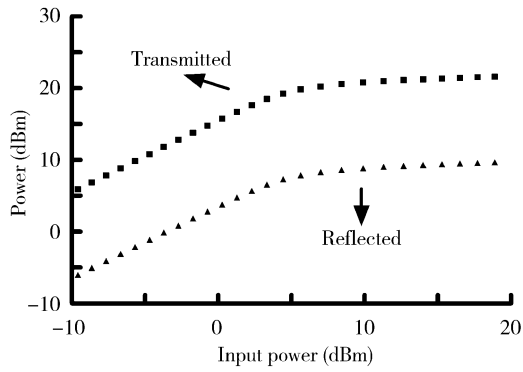


Fig. 1. Transmitted and reflected RF power measured at the output port.

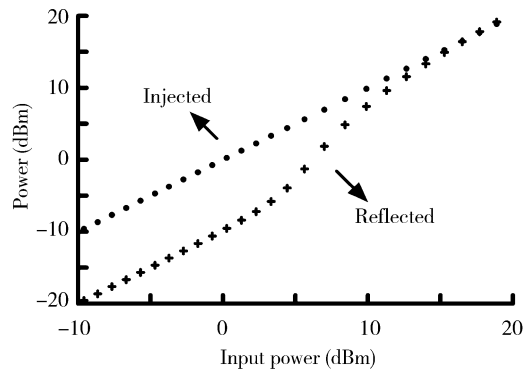


Fig. 2. Injected and reflected RF power measured at the input port.

2.2. RF power transmission at input port

The input port situation is different from the output port situation, as Figure 2 shows. On injecting a small signal sinusoidal RF signal -8.6 dBm at frequency $f_0 = 5.8$ GHz, the reflected power is about -18.2 dBm. On increasing the injection power level, the reflected power increases proportionally in the small signal range. With input power increasing from the small signal level to the large signal level, the reflected power increase becomes significant. At the -1 dB gain compression point, the injected power is about 5 dBm, and the reflected power is about -3.9 dBm. At the -3 dB gain compression point, the injected power is around 8 dBm, and the reflected power is about 4.9 dBm. At the output power saturation point, the injected power is around 16.5 dBm, and the reflected power is about 16.4 dBm.

It can be seen that the reflected power is very small at the small signal level and about 10 dB lower than the injection power. But as the input power increases from the small signal level, the reflected power deviates from the proportional line and approaches the injection power, as Figure 2 shows, which is different from the situation at the output port. After the $P_{-1\text{ dB}}$ point, the reflected power curve slope begins to become larger, and there is a knee point. The reflected power approaches the injection power curve rapidly. The reflected power becomes close to the injection power with increasing injection power at the large signal level. So at the large signal level, more power is reflected back, relatively less power gets into the transistor, the power gain is more significantly compressed, and the output

power will reach saturation. On increasing the injection power, more power will get into the transistor, but also more power is reflected back, especially at very large signal levels.

3. Discussion on power multiple frequency components

One concept is that with a sinusoidal RF signal, $a(t)$ injection as in Eq. (1), the output signal will include multiple frequency components, $\beta_0, \beta_1, \beta_2,$ and β_3 as dc, fundamental, second harmonic, and third harmonic components as shown in Eq. (2). The n th harmonic component amplitude is approximately proportional to the n th power of the input signal amplitude, A , as in Eq. (3)^[11].

$$a(t) = A \cos \omega t, \tag{1}$$

$$b(t) = \alpha_1(A \cos \omega t) + \alpha_2(A \cos \omega t)^2 + \alpha_3(A \cos \omega t)^3 = \beta_0 + \beta_1 \cos \omega t + \beta_2 \cos 2\omega t + \beta_3 \cos 3\omega t, \tag{2}$$

$$b(t) = \frac{\alpha_1 A^2}{2} + \left(\alpha_1 A + \frac{3\alpha_3 A^3}{4}\right) \cos \omega t + \frac{\alpha_2 A^2}{2} \cos 2\omega t + \frac{\alpha_3 A^3}{4} \cos 3\omega t. \tag{3}$$

However, in the realistic large signal situation, not only the transmitted signal power but also the reflected signal power by load and the reflected signal power by device contain multiple frequency components as listed in Table 1, which will be discussed in the following subsections. The percentages in the table predict the power percentages (above 0.5% as criteria) of injection power at the input port and of transmission power at the output port. The multiple frequency components of these powers are discussed at the small signal level, at the -1 dB gain compression point, at the -3 dB gain compression point, and at the saturation output power point in the following subsections.

3.1. At the small signal level

At the small signal injection level, no significant harmonic power components are observed at the input port or at the output port, as Figure 3 shows. This can be thought of as there being only fundamental injection power and reflection power at the input port and fundamental transmission power and reflection power at the output port at the small signal level.

3.2. At the -1 dB gain compression point

Increasing the injection power from the small signal level to the large signal level causes the power gain to decrease. The RF power multiple frequency components at the -1 dB gain compression point are shown in Fig. 4. So, the reflected fundamental power (12.9% of the injected fundamental power) at the input port, the reflected fundamental power (6.4% of the transmitted fundamental power) at the output port, and the transmitted second harmonic power (0.7% of the fundamental transmitted power) at the output port are the major visible factors causing power gain compression and nonlinearity at the -1 dB gain compression point.

Table 1. Forward and reflection power at input and output ports.

	Small signal (dBm)	$P_{-1\text{ dB}}$ point (dBm)	$P_{-3\text{ dB}}$ point (dBm)	Sat. power point (dBm)
Input port:				
Fundamental injection power	-8.64	5	8	16.5
Fundamental reflection power	-18.62	-3.9 (12.9%)	4.9 (50%)	16.4 (> 90%)
2nd harmonic reflection power	—	—	-2.2 (1%)	-0.88 (1.83%)
3rd harmonic reflection power	—	—	-20	-12.4
Output port:				
Fundamental transmission power	6.88	19.3	20.6	21.5
2nd harmonic transmission power	—	-2.5(0.7%)	5 (2.75%)	9.1 (5.8%)
3rd harmonic transmission power	—	-9.7	-0.11 (0.85%)	5.5 (1.2%)
Fundamental reflection power	-5.06	7.3 (6.4%)	8.6 (6.3%)	9.5 (6.4%)
2nd harmonic reflection power	—	-11.8	-4.3	-0.19
3rd harmonic reflection power	—	-15.2	-5.6	0.03

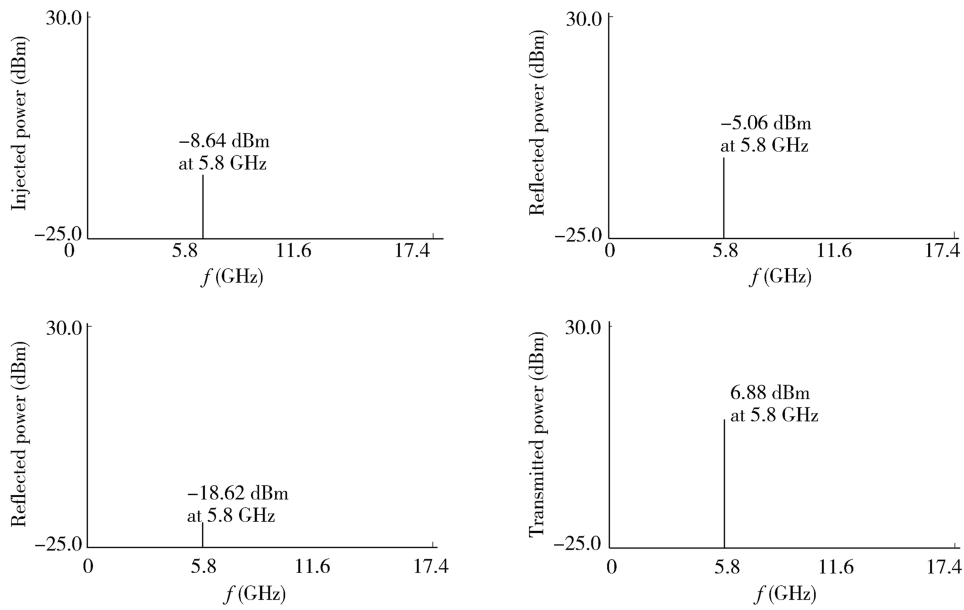


Fig. 3. RF power multiple frequency components at the input port and the output port measured at the small signal level. The left two diagrams are for the input port and the right two diagrams are for the output port.

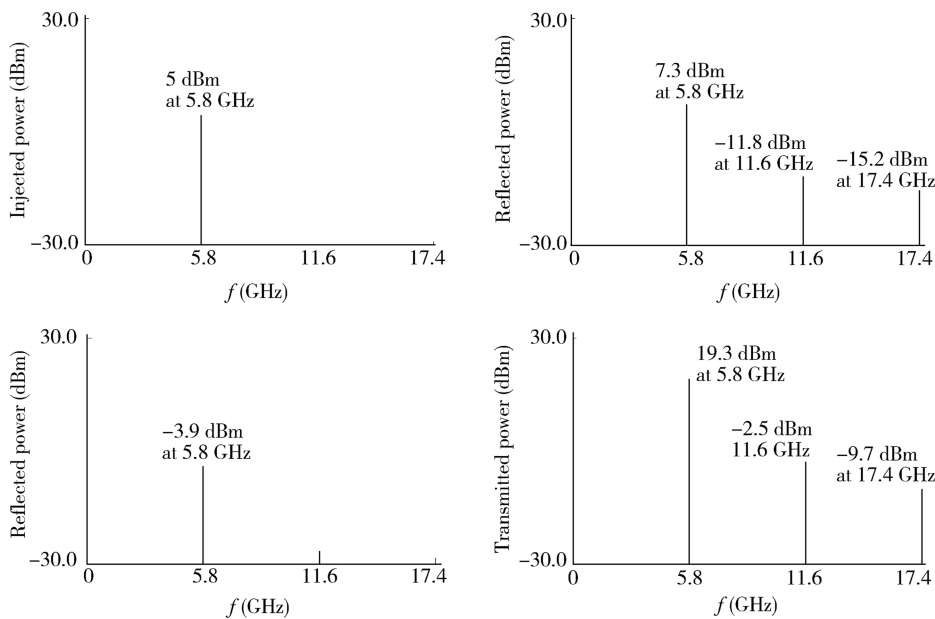


Fig. 4. RF power multiple frequency components at the input port and the output port measured at the -1 dB gain compression point. The left two diagrams are for the input port and the right two diagrams are for the output port.

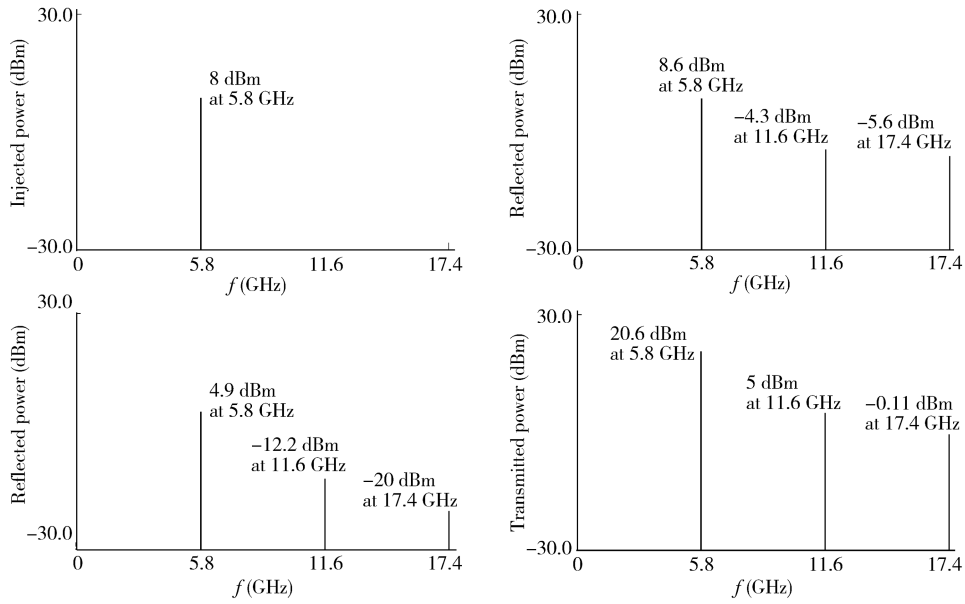


Fig. 5. RF power multiple frequency components at the input port and the output port measured at the -3 dB gain compression point. The left two diagrams are for the input port and the right two diagrams are for the output port.

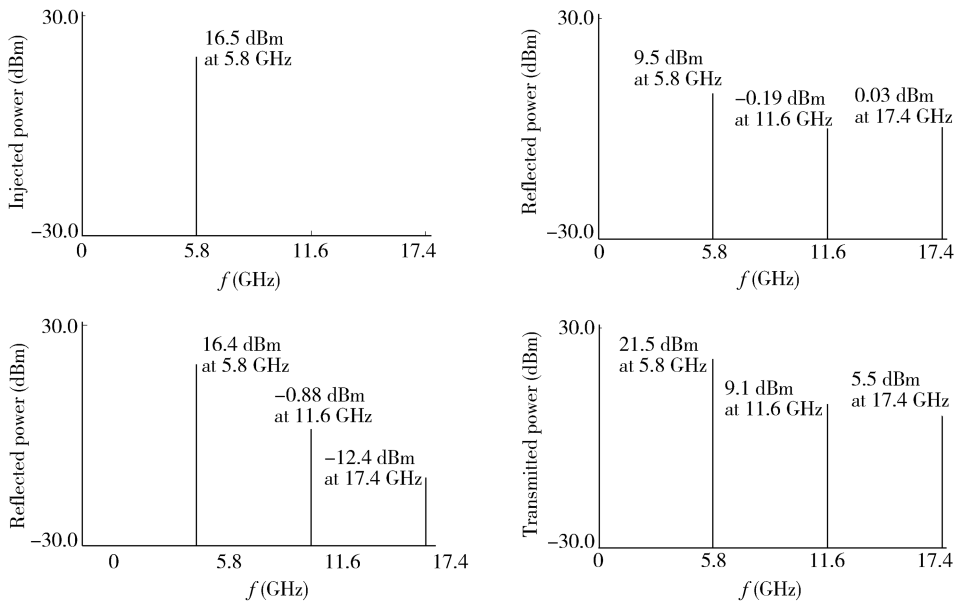


Fig. 6. RF power multiple frequency components at the input port and the output port measured at the power saturation point. The left two diagrams are for the input port and the right two diagrams are for the output port.

3.3. At the -3 dB gain compression point

Increasing the injection power continually from the -1 dB gain compression $P_{-1\text{dB}}$ point, the power gain is compressed continually. The RF power multiple frequency components are shown in Fig. 5. Compared with the situation at the -1 dB compression point, the major factors affecting power gain at the -3 dB compression point are the fundamental reflection power (50% of the injection power) and the second harmonic reflection power (1% of the injection power) at the input port; and the fundamental reflection power (6.3% of transmitted power), the second harmonic transmission power (2.75% of the transmitted power), and the third harmonic transmission

power (0.85% of the transmitted power) at the output port.

3.4. At the saturation output power point

With continual increase of the input power from the $P_{-3\text{dB}}$ point, the output power reaches maximum output power and is saturated. The RF power multiple frequency components are shown in Fig. 6. It can be seen that at the input port the reflected fundamental power is close to the injected power: much injected power has been reflected back, and this is the most significant factor causing power gain compression and output power saturation. In addition, the fundamental reflection power ($> 90\%$ of the injection power) and the second harmonic reflection power (1.83% of the injection power) at

the input port and the fundamental reflection power (6.4% of the transmitted power), second harmonic transmission power (5.8% of the transmitted power), and third harmonic transmission power (1.2% of the transmitted power) at the output port have important effects.

4. Conclusion

In this paper, the RF large signal power transmission characteristics of an advanced InGaP HBT are investigated experimentally at the small signal level, at the -1 dB gain compression point, at the -3 dB gain compression point, and at the maximum saturation output power point. The reasons for power gain compression and nonlinearity are explained.

The experimental result shows that (1) the reflected powers at the output port are in proportion to the output power increase, and about 12 dB lower than the output power not only at small signal levels but also at large signal levels. (2) However, the reflected powers at the input port are not always in proportion to the input power increase. At the small signal level, the reflected powers are about 10 dB lower than the injection power, but with injection power increasing, the power reflection is not in proportion to the injection power, and approaches the injection power level rapidly. There is a knee point for the reflection power curve after the $P_{-1\text{ dB}}$ compression point with increasing injection power. To the best of the authors' knowledge, these results have not been presented in other publications. Also, (3) with input power increasing from the small signal level, RF power gain compressions and signal distortions appear. The fundamental power reflections at the input port and at the output port are significant factors, and the following components are also important factors at the corresponding power levels: the transmitted second harmonic power at the output port at the -1 dB gain compression point; the transmitted second harmonic power and third harmonic power at the output port and the reflected second harmonic power at the input port

at the -3 dB gain compression point; the transmitted second harmonic and third harmonic power at the output port, and the reflected second harmonic power at the input port at the saturation output power point.

References

- [1] Fukuda T, Negoro N, Ujita S, et al. A 26 GHz short-range UWB vehicular-radar using 2.5 Gcps spread spectrum modulation. IEEE Microwave Symposium Digest, June 2007, 3: 1311
- [2] Cripps S. Microwave power amplifiers for wireless communications. New York: Artech House, 2006
- [3] Hattori R. Manufacturing technology of InGaP HBT power amplifiers for cellular phone applications. GaAs Mantech Digest, April 2002: 241
- [4] Sylvain H, Jean-Michel N, Raymond Q, et al. Measurement and modeling of static and dynamic breakdowns of power GaInP/GaAs HBTs. IEEE MTT-S Digest, August 2002
- [5] Groote V, Jardel O, Verspecht J, et al, Time domain harmonic load-pull of an AlGaIn/GaN HEMT. The 66th ARFTG Conference Washington, District of Columbia, USA, December 2005
- [6] Clark C J, Chrisikos G, Muha M S, et al. Time-domain envelope measurement technique with application to wideband power amplifier modeling. IEEE Trans Microw Theory Technol, 1998, 46(12): 2531
- [7] Verbeyst F, Bossche M V. Real-time and optimal PA characterization speeds up PA design. 34th European Microwave Conference Digest, Oct 2004, 10: 431
- [8] Reveyrand T, Maziere C, Nebus J M, et al. A calibrated time domain envelope measurement system for the behavioral modeling of power amplifiers. Eur Microw Week GaAs, Milan, Italy, Sep 2002, 9: 237
- [9] Agilent, Large signal network analyzer brochure, 2009
- [10] Blockley P, Gunyan V, Scott J. Mixer-based vector-corrected vector signal/network analyzer offering 300 kHz–20 GHz bandwidth and traceable phase response. IEEE International Microwave Symposium Digest, June 2005, 6: 1497
- [11] Behzad R. RF microelectronics. New York: Pearson Education Inc, 1998